



Published in final edited form as:

Eur J Med Chem. 2013 August ; 66: 114–121. doi:10.1016/j.ejmech.2013.05.021.

Ligand/kappa-Opioid Receptor Interactions: Insights from the X-Ray Crystal Structure

Karina Martinez-Mayorga¹, Kendall G. Byler², Austin B. Yongye², Marc A. Giulianotti², Colette T. Dooley², and Richard A. Houghten^{2,3}

¹Instituto de Química, UNAM, Av. Universidad 3000, México D.F.,

²Torrey Pines Institute for Molecular Studies, Port St. Lucie, FL 34987

³Torrey Pines Institute for Molecular Studies, San Diego, CA 92121, USA

Abstract

During the past five years, the three-dimensional structures of 14 different G-protein coupled receptors (GPCRs) have been resolved by X-ray crystallography. The most recently published structures, those of the opioid receptors (ORs), are remarkably important in pain modulation, drug addiction, and mood disorders. These structures, confirmed previously proposed key interactions conferring potency and antagonistic properties, including the well-known interaction with Asp138, conserved in all aminergic GPCRs. In addition, crystallization of the opioid receptors highlighted the potential function of the ECL2 and ICL2 loops. We have previously reported a set of potent and selective kappa opioid receptor peptide agonists, of which ff(D-nle)r-NH₂ is among the most potent and selective ones. These peptides were identified from the deconvolution of a 6,250,000 tetrapeptide combinatorial library. A derivative of this set is currently the subject of a phase 2 clinical trial in the United States. In this work, we describe comparative molecular modeling studies of kappa-OR peptide agonists with the co-crystallized antagonist, JD₁Tic, and also report structure-activity relationships of 23 tetrapeptides. The overall binding and contact interactions are sound and interactions known to favor selectivity and potency were observed. Additional modeling studies will reveal conformational changes that the kappa-OR undergoes upon binding to these peptide agonists.

Keywords

kappa-opioid receptor; tetrapeptide; molecular modeling; combinatorial chemistry

1. Introduction

Opioid receptors (OR) belong to Family A of the G-Protein Coupled Receptor (GPCR) superfamily. GPCRs activate signal transduction from the outside to the inside of cells. These receptors are therapeutic targets for approximately 40% of current medicinal drugs. Notably, the contributions of Dr. Robert Lefkowitz and Dr. Bryan Kobilka to the GPCR field merited the 2012 Nobel Prize in Chemistry[1]. Opioid receptors in particular, participate in many physiological processes, including pain, drug addiction and mood

© 2013 Elsevier Masson SAS. All rights reserved.

Publisher's Disclaimer: This is a PDF file of an unedited manuscript that has been accepted for publication. As a service to our customers we are providing this early version of the manuscript. The manuscript will undergo copyediting, typesetting, and review of the resulting proof before it is published in its final citable form. Please note that during the production process errors may be discovered which could affect the content, and all legal disclaimers that apply to the journal pertain.

disorders, among other diseases. Due to the therapeutic and structural relevance of the OR, intense research has been directed to understand their structure and function. The four OR subtypes, named mu, kappa, delta and the nociceptin receptor, have been crystalized this year at 2.8, 2.9, 3.4, and 3.0 Å resolution, respectively [2-5]. These three-dimensional structures allow one to investigate, at the atomic level, the structural features that promote binding affinity, selectivity and ultimately, give insights into the mechanism(s) of activation of these receptors. In addition, these three-dimensional structures can be used as templates for the development of molecular models of other GPCRs. It is expected that molecular models will help fill the gaps in the 3D structures of other GPCRs, as well as be used to investigate activation mechanisms, postulate allosteric sites, develop structure-affinity and structure-function relationships, etc.

A number of molecules have been synthesized [6] and evaluated for opioid receptor binding affinity through binding assays, as well as functional assays. The chemical structures of the ligands, as well as their associated biochemical information, can be easily obtained from public domain sources: for example from the International Union of Basic and Clinical Pharmacology (<http://www.iuphar-db.org/>), ChEMBL, PubChem, among others.

Over the years a number of opioid ligands have been identified with the deconvolution of mixture-based combinatorial libraries at the Torrey Pines Institute for Molecular Studies (TPIMS) [7-9]. Efforts have been made to integrate this mixture-based approach with computational screening [10]. Chemoinformatic studies by means of molecular scaffolds, molecular properties, and structural fingerprints show the diversity of these libraries and their uniqueness, based on: a) the partial overlap with the structural space of drugs, b) the presence of scaffolds not contained in other compound collections [11], and c) the increased molecular complexity as compared to compound libraries commonly used in high-throughput screening (HTS) programs [12].

For opioid receptor binding affinity, the scaffolds explored in these libraries include bicyclic guanidines, piperazines, triamines, and peptides of different lengths [13-15]. A particularly useful study consisted of the deconvolution of a 6,250,000 tetrapeptide combinatorial library. This library allowed the identification of potent and selective ligands for the kappa OR, with the general sequence ffr-NH₂ [16]. A derivative of this set is currently the subject of a phase 2 clinical trial.

Molecular models of small molecules [17] and peptides [18] bound to opioid receptors, are described elsewhere. Conformational preferences of cyclic peptides have also been explored [19]. With the aim of investigating the mode of action of opioid-binding peptides, cyclic analogues (e. g. pep10) have been synthesized and evaluated by Pogozeva et al [20]. For the mu-OR, potent and selective cyclic peptides were obtained [21]. However, for the kappa-OR, potency was accomplished, but selectivity remained elusive for these cyclic peptides. The binding mode derived by Pogozeva et al [20] of a potent disulfur cyclic peptide fulfills pharmacophoric features known to be important for OR binding affinity. Our understanding of GPCR function is increasing due to the crystal structures now available. It can be hypothesized that structural features that are common among the available crystal structures could be translated across other GPCRs. An interesting example is the comparison of the crystal structures of the agonist-bound β -adrenoceptors in an inactive state [22]. The structures of the thermostabilized receptors bound to a partial agonist or a full agonist were nearly identical. Moreover, the structures of the receptors were very similar to the structures when bound to antagonists. A similar goal was pursued and achieved for the β -adrenergic receptor (β_2 AR) where the agonist-bound receptor remained in the inactive form [23]. This approach can be translated to other GPCRs. For example, the report of the crystallographic structure of the kappa-OR is complemented with the molecular modeling of agonists and

antagonists into the binding pocket, including salvinorin A (SalA) analogues. SalA is a natural product described in 1982 [24] and pharmacologically characterized in 2004 [25]. The unique feature of SalA and analogues, compared to all previously known opioid ligands, is that it lacks a charged or polar nitrogen atom, known to be essential for OR binding recognition.

In this work, using the inactive state of the crystallographic structure of the kappa-OR, we explored and compared the conformational preferences of the side chains in the binding site when bound to the crystallographic ligand (an antagonist), to a potent non-selective kappa-OR cyclic peptide agonist, and to our previously reported potent and kappa-OR selective tetrapeptide agonist. Structure-activity relationship studies of 24 analogues of our kappa-OR agonists are in agreement with our model.

2. Results and Discussion

A summary of the relevant interactions involved in binding affinity, selectivity and activation of the kappa-OR, is shown in Table 1; these interactions have been identified mainly from mutagenesis studies [3].

Three kappa-OR ligands were investigated in this study; JDTic [3], pep10 [20], and ff(D-nle)r-NH₂ [16]. In order to gain some insight on the flexibility of each ligand-receptor complex, we performed a conformational search of the side chains of all the residues within 4Å to each ligand. During the searches, the ligand and the neighboring residues were free to move. A summary of residues neighboring each ligand and ligand-receptor interactions are shown in Tables 2 and 3, respectively.

2.1 Conformational search of JDTic-kappa-OR binding site

The SAR, binding interactions and pharmacophoric features of the kappa-OR co-crystallized ligand, JDTic, are described elsewhere [3]. Here we explored the conformational freedom of JDTic into the inactive state of the kappa-OR resulting in 11 conformations. Notably, except for Tyr312, Gln115 and Thr139, the conformations of the residues around JDTic remained nearly identical to those observed in the crystal structure. A graphical representation of the different conformations and the relative orientations of JDTic are shown in Figure S1A. The previously reported V-shape of JDTic observed when bound to the kappa-OR [3] was maintained in the conformational search. These conformations can be clustered into two slightly different orientations. During the conformational search, we deleted structured water molecules to explore the effect of water-mediated stabilization. Interestingly, the two binding poses obtained for JDTic differed from the reported orientation observed in the kappa-OR crystal structure, (see Figure S1B in Supplementary material) with a larger displacement on the isoquinoline side of JDTic. For pose1, shown in Figure S1C, the hydroxyl group of the isoquinoline group is able to engage in a hydrogen bonding interaction with Tyr139. In doing so, the interaction with Asp138 is now through the amide nitrogen atom, instead of the amines in the piperidine and the isoquinoline moieties, as reported [3]. The displacement obtained in pose 2, shown in Figure S1D, is more dramatic. In this pose, the isoquinoline ring makes contacts with Asp223, and the carbonyl group maintains a hydrogen bond interaction with Tyr312. Although these two putative orientations make favorable polar interactions, in both cases the interaction of the amine groups with Asp138 and the overall orientation of JDTic in the binding pocket are compromised. This underscores the importance of structured water molecules.

2.2 Conformational search of pep10-kappa-OR binding site

The conformationally constrained cyclic peptide, pep10, derived by Pogozheva et al. [20] was translated to the coordinates of the kappa-OR crystal structure. The resulting complex was then subjected to conformational search within the binding site, producing 29 conformers. The conformational space spanned by pep10 and representative conformers are shown in Figure 1A and 1B. While the hydroxyphenyl group of pep10 located at the bottom of the pocket remained unchanged, in terms of both conformation and orientation, during the conformational search, the other two phenyl rings spanned a large number of rotamers. This is an indication of the tightness at the bottom of the pocket as well as the favorable orientation of the hydroxyphenyl group of pep10. An example of the relative orientation of JDtic with pep10 is shown in Figure 1C.

As expected, the positively charged amine group makes a salt bridge with Asp138, and the hydroxyphenyl group located at the bottom of the pocket forms a hydrogen bond with His291. These two interactions serve to anchor pep10 into this region. In this model, pep10 is able to make hydrogen bond interactions with Tyr312 and Glu297. These residues have been regarded as important for kappa selectivity; substitution of Tyr312 for Trp^{7,35}, found in the mu-OR results in the loss of this polar interaction. However, pep10 binds tightly to the mu-OR. Therefore, absence of an H-bond interaction in mu was not sufficient, in and of itself, to impair the binding affinity of pep10 to mu-OR. In turn; Glu297 has been found to be relevant to kappa selectivity, particularly for morphinans. Although this interaction would enhance binding affinity to kappa-OR, it is absent in the kappa-OR crystal structure bound to JDtic, suggesting that it is not a requirement for achieving kappa selectivity.

2.3 Conformational search of ff(D-nle)r-NH₂-kappa-OR binding site

Initially, automated docking was attempted for ff(D-nle)r-NH₂ (using GLIDE). The resulting binding modes did not show the expected interactions, e. g. the salt bridge with Asp138. One of the reasons that makes automated docking of this tetrapeptide a challenging task is its high flexibility; this tetrapeptide contains 22 rotatable bonds. In contrast, typical small molecules in docking studies have up to 10 rotatable bonds [12]. In order to develop an initial orientation of ff(D-nle)r-NH₂ in the binding pocket, we used pep10 as a reference and performed a conformational search similar to that performed for JDtic and pep10. For comparison, the relative orientation of ff(D-nle)r-NH₂ and JDtic is shown in Figure 2A, and to pep10, shown in Figure 2B. The relatively good alignment of ff(D-nle)r-NH₂ and pep10 and the presence of important interactions within the kappa-OR binding site gave a level of confidence to the binding model of ff(D-nle)r-NH₂. To note, while ff(D-nle)r-NH₂ is a selective kappa binder, pep10 is not. Therefore, it is expected that interactions promoting selectivity to kappa-OR should be present in ff(D-nle)r-NH₂ but absent in pep10. The conformational search of ff(D-nle)r-NH₂ within the kappa-OR binding site produced 34 very similar conformers. The orientation obtained allows the characteristic salt bridge with Asp138 and the localization of a phenyl ring at the bottom of the pocket. A number of other favorable interactions were also present, and are summarized in Table 3. Similarly to pep10, ff(D-nle)r-NH₂ makes H-bond interactions to Lys227, Glu297 and Tyr312. However, while pep10 interacts weakly with Glu209 via π -H contacts, ff(D-nle)r-NH₂ makes strong H-bond and ionic interactions with this residue, located in the ECL2. Polar interactions with Glu209 appear to be promoting the kappa-OR subtype selectivity of ff(D-nle)r-NH₂. It is worth stressing that peptide-binding receptors crystallized to date (opioid receptors and CXCR4) reveal that the ECL2 forms a π -hairpin structure, believed important for recognition and selectivity [26].

Lastly, our conformational search of the side chains in the binding pocket shows that ff(D-nle)r-NH₂ favors the side chain rotation of Trp287, located at the bottom of the pocket.

Experimental studies [27] indicate that Trp^{6.48} is a key residue in GPCR activation. Figure 3 shows the orientation of Trp287 in the crystallographic structure (green) and in the ff(D-nle)r-NH₂ model. In the presence of JD_{Tic}, the isopropyl group locks the orientation of Trp287 making hydrophobic interactions. Meanwhile, ff(D-nle)r-NH₂ favors the side chain rotation of Trp287, most likely enhancing its agonist behavior. This subtle structural difference is the subject of discussion in regard to kappa-OR agonists versus antagonists [3]. Activation of GPCRs conveys changes in the orientation of the transmembrane helices (Supplementary Table S1). For example, the all-atom rmsd for rhodopsin when comparing the dark or inactive state (PDBID: 1U19) to the light or activated state (PDBID:3PQR) is 3.07 Å. Changes in the binding pocket are less pronounced (rmsd 1.75 Å). Moreover, the all-atom rmsd after alignment of TMs 1, 2, and 4 (thought to move less upon activation) increases to 6.5 Å. The same trend is observed when comparing the kappa-OR crystal structure with a publicly available homology model of kappa-OR in a modeled activated state (Supplementary Table S1). This illustrates how small changes in the binding pocket lead to large changes in the conformation of the receptor.

2.4 Structure activity relationships for ff(D-nle)r-NH₂ analogues

The model obtained for ff(D-nle)r-NH₂ was then used as a template to analyze tetrapeptides obtained from the same combinatorial library [16]. We have previously reported the side chains and the corresponding K_i values for each tetrapeptide, they are summarized in Table 4 [16]. Clearly, incorporation of a tryptophan side chain in the R3 position conducted to peptides with K_i values greater than 1000nM. Another clear pharmacophoric feature is the presence of an arginine group in the R4 position, this group conducted to the best kappa-OR binders of the series.

Taking ff(D-nle)r-NH₂ as a reference, 3D overlays of each peptide were performed, similarity values are summarized in Table 4. Overlays are graphically represented in Table 5, along with average K_i and 3D similarity values divided into three groups. These overlays are based on common pharmacophoric features to the reference peptide and do not consider any spatial restrains from the receptor. Not surprisingly the most active tetrapeptides (molecules 2-8) have overall higher similarity to ff(D-nle)r-NH₂ compared to the two other groups; molecules 9-16 and 17-24.

The importance of the R3 and R4 positions can be graphically and numerically compared with the tree shown in Figure 4. Based on K_i values, the first split corresponds to the R3 position, where the average K_i values for peptides with R3=W is 5575 and for R3 W is 43.9. The next split corresponds to the R4 position, where in all cases (nodes 4-7), the arginine side chain is preferred. The average K_i values are lower when R4=r than R4=D-cha. The last split (terminal nodes 8-11) corresponded to R3 and R1 for nodes 6 and 7, respectively. For node 6, molecules 9-16, nle consistently conducted to better kappa-OR binders. However, for the most active tetrapeptides (node 7) the average K_i for R1=r or R1=nle did not differ significantly: 3.6 and 4.3nM, respectively.

The drastic drop in activity when R3=W shows that this position cannot allocate this substituent while maintaining the biologically significant orientation of the remaining groups into the kappa-OR binding pocket. Importantly, peptides with the arginine group at the R4 position, and with R3 W, not only were the most active but also the most selective ones [16]. According to our model, described above, the presence of an arginine group in the R4 position allows strong H-bond and ionic interactions with Glu209, which are important for kappa-OR selectivity, in agreement with our model.

This study exemplifies the feasibility of modeling a kappa-OR peptide agonist into the crystallographic structure obtained in the inactive state. The overall binding and contact

interactions are sound, and the hypothesis is supported by crystallographic structures of agonist-bound receptors obtained in the inactive state [22, 23].

3. Conclusions

Molecular modeling studies were conducted for the kappa-OR co-crystallized antagonist and for selective and non-selective peptide agonists using the recently published crystallographic structure of the kappa-OR (in the active state). The orientation of the ligands in the kappa-OR binding site is in agreement with interactions known to promote binding affinity and selectivity. In particular, strong interactions with Glu209, located in the ECL2, were observed for the selective peptide agonist. This interaction appears to be enhancing kappa selectivity. In addition, the selective peptide agonist studied here, ff(D-nle)r-NH₂, promoted rotation of the Trp287 side chain, known to be involved in GPCR activation. Structure-activity relationships derived for 23 tetrapeptides obtained from the same combinatorial library underscored the importance for an arginine side chain towards Glu209 and the drop in activity when incorporating a tryptophan group at the R3 position. The knowledge-driven modeling approach employed here produced sound models and can be expanded to conformational studies of other relevant opioid receptor ligands.

4. Methods

Data collection

Atomic coordinates of rhodopsin in the inactive (PDBID: 1U19) and active (PDBID: 3PQR) states, as well as of the kappa-OR in the inactive form (PDBID: 4DJH) were downloaded from the Protein Data Bank (PDB). A homology model of the kappa-OR and the atomic coordinates of the peptide modeled by Pogozheva et al (pep10) were downloaded from <http://mosberglab.phar.umich.edu/resources/>. Translation to the same coordination frame of the active and inactive form of each receptor and rmsd calculations were performed with Chimera [28]. The missing intracellular loop in the X-ray structure of the kappa-OR was introduced and modeled with Maestro [29].

Conformational searches

The conformational searches were performed in Macromodel (Schrödinger Inc.) using the OPLS-2005 force field and GB/SA water model (in the presence of the receptor). The ligands were free to rotate, translate and change conformation during the conformational search. Residues within a radius of 4Å to the ligand were also free to change conformation. For all the residues in this layer, constrained-atom mutual interactions were calculated. An additional shell of 5Å was set from the first layer; residues on this layer were not allowed to move. The remainder of the protein was ignored. The energy minimization was performed using the Polak-Ribier Conjugate Gradient (PRCG) method [30]. Default settings were employed for convergence (gradient, threshold of 0.05) for up to 500 iterations. The conformational search was sampled using the “mixed torsional/large-scale-low-mode” method. Torsion sampling options were set to intermediate, retaining mirror-image conformations. The maximum number of steps was 200. The energy window for saving structures was 21.0 kJ/mol. Redundant conformers were eliminated using a maximum atom deviation cutoff of 0.5Å. The resulting complexes were clustered based on atomic rmsd of the ligands and neighboring residues within 4Å of the ligand. The similarity rmsd matrix was clustered using a complete linkage method, and the number of clusters was chosen using the Kelley penalty function [31, 32]. The centroid of each cluster was selected to represent each cluster. The final complexes were analyzed with Maestro 9.3 [29].

3D alignments and similarity values

3D overlays were performed within MarvinSketch 5.11.4 by ChemAxon. The “align by pharmacophore type” option was used and the flexible alignment was lunched for 40 initial conformations. This 3D alignment protocol searches for matching of H-bond donors, acceptors, aromatic and hydrophobic groups, as well as positive and negative charges, the similarity values correspond to the Tanimoto coefficient.

Supplementary Material

Refer to Web version on PubMed Central for supplementary material.

Acknowledgments

This work was supported by the State of Florida, Executive Officer of the Governor’s Department of Economic Opportunity and funded, in part, by NIDA DA031370. We would like to thank ChemAxon (<http://www.chemaxon.com>) and StatSoft for kindly providing an academic license of their software. KMM thanks DGAPA-UNAM (PAPIIT IA200513-2).

References

1. [21 Nov 2012] The Nobel Prize in Chemistry 2012, N. o.. http://www.nobelprize.org/nobel_prizes/chemistry/laureates/2012/
2. Manglik A, Kruse AC, Kobilka TS, Thian FS, Mathiesen JM, Sunahara RK, Pardo L, Weis WI, Kobilka BK, Granier S. Crystal structure of the mu-opioid receptor bound to a morphinan antagonist. *Nature*. 2012; 485:321–U170. [PubMed: 22437502]
3. Wu HX, Wacker D, Mileni M, Katritch V, Han GW, Vardy E, Liu W, Thompson AA, Huang XP, Carroll FI, Mascarella SW, Westkaemper RB, Mosier PD, Roth BL, Cherezov V, Stevens RC. Structure of the human kappa-opioid receptor in complex with JD1c. *Nature*. 2012; 485:327–U369. [PubMed: 22437504]
4. Granier S, Manglik A, Kruse AC, Kobilka TS, Thian FS, Weis WI, Kobilka BK. Structure of the delta-opioid receptor bound to naltrindole. *Nature*. 2012; 485:400–U171. [PubMed: 22596164]
5. Thompson AA, Liu W, Chun E, Katritch V, Wu HX, Vardy E, Huang XP, Trapella C, Guerrini R, Calo G, Roth BL, Cherezov V, Stevens RC. Structure of the nociceptin/orphanin FQ receptor in complex with a peptide mimetic. *Nature*. 2012; 485:395–U150. [PubMed: 22596163]
6. Alvarado C, Guzman A, Diaz E, Patino R. Synthesis of Tramadol and Analogues. *J. Mex. Chem. Soc.* 2005; 49:324–327.
7. Houghten RA, Pinilla C, Giulianotti MA, Appel JR, Dooley CT, Nefzi A, Ostresh JM, Yu YP, Maggiora GM, Medina-Franco JL, Brunner D, Schneider J. Strategies for the use of mixture-based synthetic combinatorial libraries: Scaffold ranking, direct testing, in vivo, and enhanced deconvolution by computational methods. *J. Comb. Chem.* 2008; 10:3–19. [PubMed: 18067268]
8. Houghten RA, Pinilla C, Appel JR, Blondelle s. E. Dooley CT, Eichler J, Nefzi A, Ostresh JM. Mixture-based synthetic combinatorial libraries. *J. Med. Chem.* 1999; 42:3743–3778. [PubMed: 10508425]
9. Pinilla C, Appel JR, Borrás E, Houghten RA. Advances in the use of synthetic combinatorial chemistry: mixture-based libraries. *Nat. Med.* 2003; 9:118–122. [PubMed: 12514724]
10. Yongye AB, Pinilla C, Medina-Franco JL, Giulianotti MA, Dooley CT, Appel JR, Nefzi A, Scior T, Houghten RA, Martinez-Mayorga K. Integrating computational and mixture-based screening of combinatorial libraries. *J. Mol. Model.* 2011; 17:1473–1482. [PubMed: 20853183]
11. Singh N, Guha R, Giulianotti MA, Pinilla C, Houghten RA, Medina-Franco JL. Chemoinformatic Analysis of Combinatorial Libraries, Drugs, Natural Products, and Molecular Libraries Small Molecule Repository. *J. Chem. Inf. Model.* 2009; 49:1010–1024. [PubMed: 19301827]
12. Lopez-Vallejo F, Giulianotti MA, Houghten RA, Medina-Franco JL. Expanding the medicinally relevant chemical space with compound libraries. *Drug Discovery Today*. 2012; 17:718–726. [PubMed: 22515962]

13. Martinez-Mayorga K, Medina-Franco JL, Giulianotti MA, Pinilla C, Dooley CT, Appel JR, Houghten RA. Conformation-opioid activity relationships of bicyclic guanidines from 3D similarity analysis. *Bioorg. & Med. Chem.* 2008; 16:5932–5938. [PubMed: 18468907]
14. Yongye AB, Appel JR, Giulianotti MA, Dooley CT, Medina-Franco JL, Nefzi A, Houghten RA, Martinez-Mayorga K. Identification, structure-activity relationships and molecular modeling of potent triamine and piperazine opioid ligands. *Bioorg. & Med. Chem.* 2009; 17:5583–5597. [PubMed: 19576786]
15. Yongye, AB.; Martinez-Mayorga, K. Molecular Aspects of Opioid Receptors and Opioid Receptor Painkillers. In: Racz, Gabor B.; Noe, CE., editors. *Pain Management - Current Issues and Opinions*. InTech; 2012.
16. Dooley CT, Ny P, Bidlack JM, Houghten RA. Selective ligands for the mu, delta, and Kappa opioid receptors identified from a single mixture based tetrapeptide positional scanning combinatorial library. *J. Biol. Chem.* 1998; 273:18848–18856. [PubMed: 9668060]
17. Gentilucci L, Tolomelli A, De Marco R, Artali R. Molecular Docking of Opiates and Opioid Peptides, a Tool for the Design of Selective Agonists and Antagonists, and for the Investigation of Atypical Ligand-Receptor Interactions. *Curr. Med. Chem.* 2012; 19:1587–1601. [PubMed: 22376035]
18. Eguchi M. Recent advances in selective opioid receptor agonists and antagonists. *Med. Res. Rev.* 2004; 24:182–212. [PubMed: 14705168]
19. Yongye AB, Li YM, Giulianotti MA, Yu YP, Houghten RA, Martinez-Mayorga K. Modeling of peptides containing D-amino acids: implications on cyclization. *J. Comp.-Aid. Mol. Des.* 2009; 23:677–689.
20. Przydzial MJ, Pogozheva ID, Ho JC, Bosse KE, Sawyer E, Traynor JR, Mosberg HI. Design of high affinity cyclic pentapeptide ligands for μ -opioid receptors. *J. Pep. Res.* 2005; 66:255–262.
21. Mosberg HI, Fowler CB. Development and validation of opioid ligand-receptor interaction models: the structural basis of mu vs. delta selectivity. *J. Pep. Res.* 2002; 60:329–335.
22. Warne T, Moukhametzianov R, Baker JG, Nehme R, Edwards PC, Leslie AGW, Schertler GFX, Tate CG. The structural basis for agonist and partial agonist action on a beta(1)-adrenergic receptor. *Nature.* 2011; 469:241–244. [PubMed: 21228877]
23. Rosenbaum DM, Zhang C, Lyons JA, Holl R, Aragao D, Arlow DH, Rasmussen SGF, Choi HJ, DeVree BT, Sunahara RK, Chae PS, Gellman SH, Dror RO, Shaw DE, Weis WI, Caffrey M, Gmeiner P, Kobilka BK. Structure and function of an irreversible agonist-beta(2) adrenoceptor complex. *Nature.* 2011; 469:236–240. [PubMed: 21228876]
24. Ortega A, J.F. B, Manchad PS. Salvinorin, a New trans-Noclerodane Diterpene from *Salvia divinorum* (Labiatae). *J. Chem. Soc. Perkin Trans.* 1982:2505–2508.
25. Roth BL, Baner K, Westkaemper R, Siebert D, Rice KC, Steinberg S, Ernsterberger P, Rothman RB. Salvinorin A: A potent naturally occurring nonnitrogenous μ opioid selective agonist. *Proc. Natl. Acad. Sci. USA.* 2002; 99:11934–11939. [PubMed: 12192085]
26. Wang JB, Johnson PS, Wu JM, Wang WF, Uhl GR. Human kappa-opiate receptor 2nd extracellular loop elevates dynorphins affinity for human mu/kappa chimeras. *J. Biol. Chem.* 1994; 269:25966–25969. [PubMed: 7929306]
27. Standfuss J, Edwards PC, D'Antona A, Fransen M, Xie GF, Oprian DD, Schertler GFX. The structural basis of agonist-induced activation in constitutively active rhodopsin. *Nature.* 2011; 471:656–660. [PubMed: 21389983]
28. Pettersen EF, Goddard TD, Huang CC, Couch GS, Greenblatt DM, Meng EC, Ferrin TE. UCSF Chimera-A Visualization System for Exploratory Research and Analysis. *J. Comput. Chem.* 2004; 25:1605–1612. [PubMed: 15264254]
29. Maestro 9.1. Schrödinger, LLC; New York, NY: 2010.
30. Polak E, Ribiere G. Note on Convergence of Conjugate Direction Methods *Revue Francaise D Informatique de Recherche Operationnelle.* 1969; 3:35.
31. Kelley LA, Gardner SP, J. SM. An automated approach for clustering an ensemble of NMR-derived protein structures into conformationally related subfamilies. *Prot. Engineering.* 1996; 9:1063–1065.

32. Yongye AB, Bender A, Martinez-Mayorga K. Dynamic clustering threshold reduces conformer ensemble size while maintaining a biologically relevant ensemble. *J. Comput.-Aided Mol. Des.* 2010; 24:675–686. [PubMed: 20499135]

Highlights

- * Agonist and antagonist tetrapeptides were analyzed in the inactive conformation of the kappa-OR crystal structure
- * Model developed highlights the importance of polar and H-bond interactions of selective kappa-OR tetrapeptides with Glu209, located in the ECL2.
- * Rotation of Trp287, important for GPCR's activation, was observed in the model of our tetrapeptide agonist.

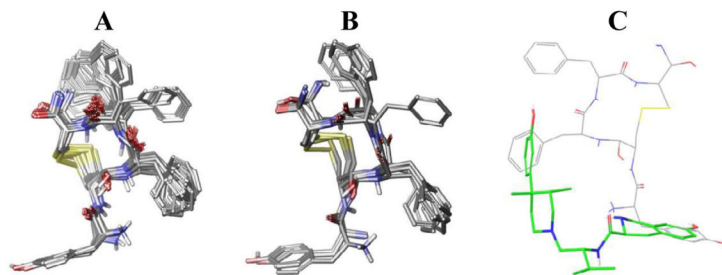


Figure 1.

A) Conformations of pep10 from the conformational search, B) representative conformations after conformer clustering procedure. C) Relative orientation of JDtic (green) and pep10 (grey) into kappa-OR binding pocket. The structure of JDtic corresponds to the one in the crystal structure (PDBID: 4DJH).

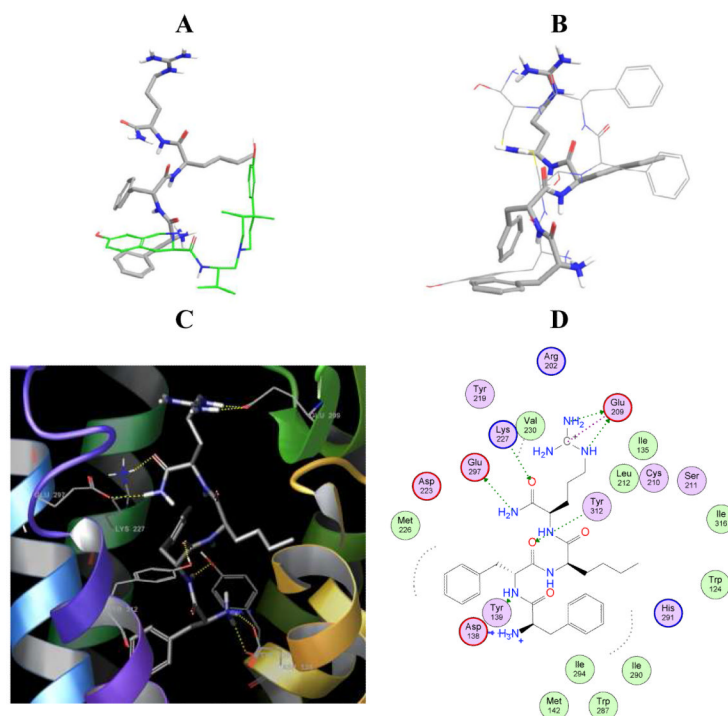


Figure 2. Relative orientation of ff(D-nle)r-NH₂ (grey thick sticks) to A) JDtIc (green) and B) pep10 (tin sticks) into the kappa-OR binding pocket. The structure of JDtIc corresponds to the one in the crystal structure (PDBID: 4DJH). Orientation C) and contact interactions D) of ff(D-nle)r-NH₂ into the kappa-OR binding site.

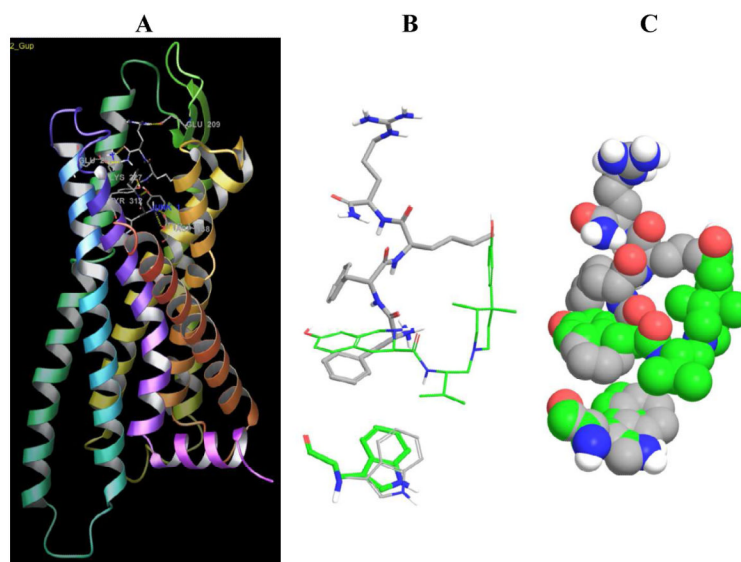


Figure 3. Effect of ff(D-nle)r-NH₂ in Trp287

Panel A) shows the overall structure of the kappa-OR, showing the binding model of ff(D-nle)r-NH₂, relevant residues are labeled. B) and C) Comparison of the orientation of Trp in the presence of the antagonist crystallographic ligand, JDtic, shown in green, and the agonist tetrapeptide ff(D-nle)r-NH₂, shown in gray.

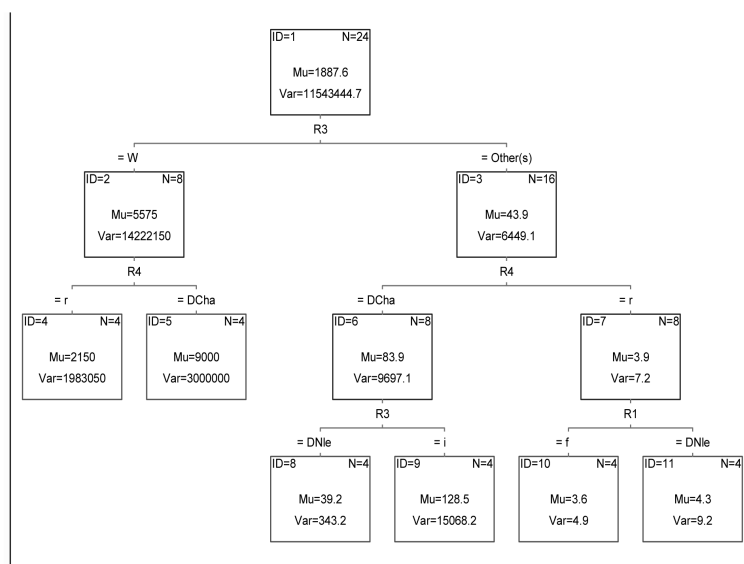


Figure 4. Classification tree for 24 tetrapeptides based on K_i values

Each split classifies molecules based on K_i values. Nodes are identified by ID numbers.

Average and variance of K_i values at each node are denoted by μ and Var values. Number of members on each node is denoted by N .

Table 1

Important interactions in the kappa-OR orthosteric binding site

Interacting residues	Type of interaction	Notes
Potency		
Asp138	Salt bridge	Conserved residue among aminergic GPCRs
Selectivity to kappa-OR		
Val108	Hydrophobic	
Val118	Hydrophobic	Based on JDTic Interactions consistent with mutagenesis and SAR studies
Ile294	Hydrophobic	
Tyr312	Hydrophobic / polar	
Selectivity to kappa-OR		
Glu297	Salt bridge at the entrance of the binding pocket	Based on morphinans. Message - address concept. Interactions consistent with mutagenesis studies
Ile294	Hydrophobic	Based on morphinans. Interactions consistent with mutagenesis studies
Glu209	Polar	Based on morphinans. Interactions consistent with mutagenesis studies.
Ser211	Polar	Located at the ECL2, interactions found in nor-BNI
Agonism/antagonism		
Trp287	Hydrophobic	Key residues in the message-address concept.
His291	Hydrophobic	
ECL2		Deemed important for ligand recognition and selectivity.
D/ERY motif	Salt bridge Arg3.5 to: Thr2736.34 (kappa); Asp/Glu6.30 (mu, delta)	<i>Ionic lock</i> of TM3 and TM6 thought to stabilize the inactive conformation. Located at the cytoplasmic end of TM3.
NPXXY motif		<i>Molecular switch</i> associated with GPCR activation. Located at the cytoplasmic side of TM7.

Table 2

Residues within 4Å to ligand; key residues are in bold, residues important for kappa-OR selectivity are underlined

	hydrophobic	acidic	basic	Polar
JDtic X-Ray structure	Val108 , Val118 , Trp124, Val134, Ile135, Met142, Ile209, Val230, Trp287 , Ile294 , Ile316	Asp138	Lys227, His291	Thr111, Gln115, Tyr139, Cys210, Tyr312 , Gly319, Tyr320
Pep10	Val118 , Trp124, Val 134, Ile135, Met142, Ile208, Val230, Ile290, Ile294 , Leu309	Asp138 , Glu209 , Glu297	Lys227, His291	Tyr139, Cys210, Tyr312
ff(D-Nle)r-NH ₂	Trp124, Ile135, Met142, Leu212, Met226, Val230, Trp287 , Ile290, Ile294 , Ile316	Asp138 , Glu209 , Asp223, Glu297	Arg202, Lys227, His291	Tyr139, Cys210, Ser211 , Tyr219, Tyr312

Table 3Ligand-receptor interactions observed for pep10 and ff(D-nle)r-NH₂

Ligand *	Receptor *	Interactions	distance	E (kcal/mol)	Importance
pep10					
N 1	ID2 Asp138 (A)	H-donor	2.54	-1.0	
N 1	OD2 Asp138 (A)	ionic	3.22	-8.4	
6-ring	CA Glu209 (A)	pi-H			selectivity
6-ring	CG Glu209 (A)	pi-H			
SG 81	NZ Lys227 (A)	H-acceptor	3.22	-1.7	
OH 12	ND1 His291 (A)	H-acceptor	2.89	-0.9	
O 79	OE2 Glu297 (A)	H-donor	2.67	-1.4	selectivity
6-ring	CG1Ile294 (A)	pi-H			
O 27	OH Tyr312 (A)	H-acceptor	2.67	-3.8	selectivity
ff(D-nle)r-NH₂					
N1 1	O Asp138 (A)	H-donor	2.75	-0.9	
N1 1	OD1 Asp138 (A)	ionic	2.80	-0.9	
N1 1	OD2 Asp138 (A)	ionic	2.80	-8.3	
N23 23	OH Tyr139 (A)	H-donor	2.98	-0.5	
N69 69	OE1 Glu209 (A)	H-donor	2.62	-1.1	selectivity
N72 72	OE2 Glu209 (A)	H-donor	2.63	-1.4	
C70 70	OE1 Glu209 (A)	ionic	2.80	-2.2	
C70 70	OE2 Glu209 (A)	ionic	2.80	-1.8	
O65 65	NZ Lys227 (A)	H-acceptor	2.80	-1.0	
N86 86	OE2 Glu297 (A)	H-donor	3.21	-1.1	selectivity
O26 26	OH Tyr312 (A)	H-acceptor	2.76	-1.1	selectivity

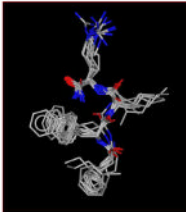
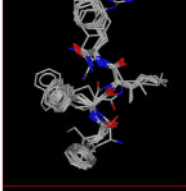
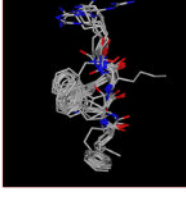
* PDB atom nomenclature

Table 4Ki values for tetrapeptides studied here and 3D similarity to reference peptide ff(D-nel)r-NH₂

	Ki (nM)	R1	R2	R3	R4	3D similarity to mol1
1	1.2	f	f	nle	r	1
2	1.5	nle	nal	i	r	0.623
3	2.3	nle	nal	nle	r	0.561
4	2.4	f	f	i	r	0.807
5	3.6	f	nal	i	r	0.646
6	4.2	nle	f	nle	r	0.588
7	7.1	f	nal	nle	r	0.715
8	9.3	nle	f	i	r	0.647
9	26	f	f	nle	cha	0.774
10	27	nle	nal	nle	cha	0.542
11	33	f	nal	nle	cha	0.601
12	53	f	nal	i	cha	0.596
13	56	nle	nal	i	cha	0.562
14	64	f	f	i	cha	0.745
15	71	nle	f	nle	cha	0.587
16	341	nle	f	i	cha	0.564
17	1140	f	f	W	r	0.598
18	1150	f	nal	W	r	0.514
19	1760	nle	nal	W	r	0.514
20	4550	nle	f	W	r	0.452
21	6000	f	nal	W	cha	0.53
22	10000	nle	f	W	cha	0.566
23	10000	f	f	W	cha	0.555
24	10000	nle	nal	W	cha	0.495

Table 5

3D overlay to reference peptide ff(D-nel)r-NH2 classified into three groups by activity

Molecules aligned to molecule 1	Average Ki (nM)	Average 3D similarity to molecule 1
<p>2-8 Common pharmacophore to active peptides: R4=r and R3 W</p> 	3.95	0.71
<p>9-16 Common pharmacophore to middle active peptides: R4=cha and R3 W</p> 	83.87	0.60
<p>17-24 Common pharmacophore to inactive peptides R3=W regardless R1,R2 and R4</p> 	5575	0.53